Regulation of Myosin-IIA Assembly and Mts1 Binding by Heavy Chain Phosphorylation †

ARTICLE *in* BIOCHEMISTRY · JUNE 2005

Impact Factor: 3.02 · DOI: 10.1021/bi0500776 · Source: PubMed

4 AUTHORS, INCLUDING:

Vladimir N Malashkevich
Albert Einstein College of Medicine
81 PUBLICATIONS **2,933** CITATIONS
SEE PROFILE

Steven Almo
Albert Einstein College of Medicine
327 PUBLICATIONS **10,355** CITATIONS
SEE PROFILE

Anne R Bresnick
Albert Einstein College of Medicine
77 PUBLICATIONS **3,436** CITATIONS
SEE PROFILE

Regulation of Myosin-IIA Assembly and Mts1 Binding by Heavy Chain Phosphorylation†

Natalya G. Dulyaninova, Vladimir N. Malashkevich, Steven C. Almo, and Anne R. Bresnick*

Department of Biochemistry, Albert Einstein College of Medicine, 1300 Morris Park Avenue, Bronx, New York 10461

Received January 13, 2005; Revised Manuscript Received March 14, 2005

ABSTRACT: Previous studies suggested that heavy chain phosphorylation regulates non-muscle myosin-II assembly in an isoform-specific manner, affecting the assembly of myosin-IIB, but not myosin-IIA. We re-examined the effects of heavy chain phosphorylation on myosin-IIA filament formation and also examined mts1 binding. We demonstrated that heavy chain phosphorylation by either protein kinase C (PKC) or casein kinase 2 (CK2) inhibits the assembly of myosin-IIA into filaments. PKC phosphorylation had no affect on mts1 binding, but CK2 phosphorylation decreased the affinity of mts1 for the myosin-IIA rod by approximately 6.5-fold. Mts1 destabilized PKC-phosphorylated myosin-IIA filaments and inhibited the assembly of myosin-IIA monomers with maximal inhibition of assembly and promotion of disassembly occurring at a molar ratio of one mts1 dimer per myosin-IIA rod. At this molar ratio, mts1 only weakly disassembled CK2-phosphorylated myosin-IIA filaments and weakly inhibited the assembly of CK2-phosphorylated myosin-IIA monomers. These observations demonstrate that CK2 phosphorylation of the myosin-IIA heavy chain protects against mts1-induced filament disassembly and inhibition of assembly, and suggest that heavy chain phosphorylation provides an additional level of regulation for the mts1−myosin-IIA interaction.

Vertebrate non-muscle cells express at least three myosin-II heavy chain isoforms denoted as A−C (*1*−*4*). Most tissues express all three isoforms (*4*); however, some cell types selectively express a single isoform. For example, platelets, lymphocytes, neutrophils, and brush border cells express only myosin-IIA (*5*), whereas testis and neuronal tissue are highly enriched in myosin-IIB (*4*, *6*). In addition, within a single cell type, myosin-IIA and myosin-IIB exhibit distinct patterns of localization (*5*, *7*), suggesting that the two isoforms have unique functional roles in vivo. Consistent with this proposal, myosin-IIA and myosin-IIB display distinct enzymatic properties (*8*−*10*).

The enzymatic activity of smooth muscle and vertebrate non-muscle myosin-II is regulated by phosphorylation on the regulatory light chain (RLC).[1] Phosphorylation of Ser19 enhances the actin-activated ATPase activity of myosin-II (*11*) and is essential for the movement of actin filaments (*12*). In addition, heavy chain phosphorylation is thought to regulate non-muscle myosin-II assembly in an isoform-specific manner. In vitro, PKC phosphorylates myosin-IIA on a single serine near the C-terminal end of the coiled coil and myosin-IIB on multiple serines in the nonhelical tailpiece (*13*, *14*), whereas casein kinase II phosphorylates both isoforms on the nonhelical tailpiece (*15*, *16*). Previous studies have suggested that heavy chain phosphorylation by either PKC or casein kinase II inhibits myosin-IIB assembly; however, in these studies, myosin-IIA assembly was unaffected by heavy chain phosphorylation (*13*, *16*).

Mts1 or S100A4, which is a member of the S100 family of Ca^{2+}-binding proteins, has been shown to preferentially bind and regulate the monomer−polymer equilibrium of myosin-IIA (*17*). Although mts1 is expressed in normal tissues, high levels of expression are observed in highly motile cells such as macrophages, lymphocytes, and neutrophils (*18*). In addition, mts1 overexpression in tumor cells has been shown to confer a metastatic phenotype (*19*, *20*). The mts1 binding site maps to residues 1909−1924 in the C-terminal end of the coiled coil of the myosin-IIA heavy chain (*17*, *21*). Furthermore, contained within the mts1 binding site is the PKC phosphorylation site at Ser1917 (*14*) and adjacent to the mts1 binding site is the CK2 phosphorylation site at Ser1944 (*13*). Several studies have shown that mts1 binding inhibits phosphorylation of the myosin-IIA heavy chain by both PKC and CK2 (*21*, *22*). This observation has led to the proposal that myosin-IIA heavy chain phosphorylation may be a mechanism for modifying the binding of myosin-II regulatory molecules such as mts1.

To further characterize the regulation of myosin-IIA by mts1, we examined the effects of heavy chain phosphorylation on mts1 binding. Our studies demonstrate that heavy chain phosphorylation modulates myosin-IIA filament assembly and also show that CK2 phosphorylation of the myosin-IIA heavy chain protects against mts1-induced filament disassembly and inhibition of assembly. These findings suggest that heavy chain phosphorylation provides an additional level of regulation for the mts1−myosin-IIA interaction.

† This work was supported by National Institutes of Health Grant GM069945.

* To whom correspondence should be addressed. Telephone: (718) 430-2741. Fax: (718) 430-8565. E-mail: bresnick@aecom.yu.edu.

[1] Abbreviations: GST, glutathione *S*-transferase; MIIA, myosin-IIA; ACD, assembly competence domain; RLC, regulatory light chain; PKC, protein kinase C; CK2, casein kinase 2; DSS, disuccinimidylsuberate.

10.1021/bi0500776 CCC: $30.25
Published on Web 04/15/2005

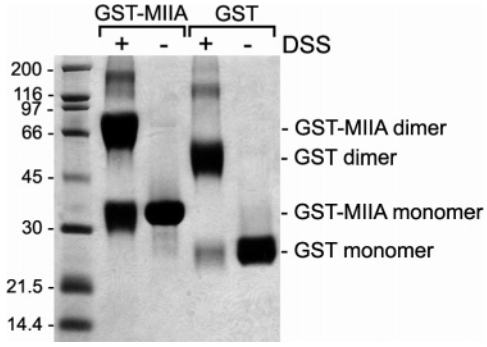

FIGURE 1: Chemical cross-linking of GST−$MIIA_{1900-1961}$. Coomassie-stained SDS−PAGE of untreated and cross-linked GST−$MIIA_{1900-1961}$ and the GST control. Monomeric GST−$MIIA_{1900-1961}$ and the GST control have apparent molecular masses of ~33.5 and ~26.8 kDa, respectively. The addition of the bifunctional cross-linker DSS resulted in the appearance of prominent bands at ~70 and 55 kDa, consistent with the formation of GST dimers. Minor bands with apparent molecular masses of ~140 and ~120 kDa were detected in the cross-linked samples, indicating insignificant tetramer assembly.

EXPERIMENTAL PROCEDURES

Molecular Modeling and Electrostatic Surface Potential Calculations. Residues 1730−1928 from the two-stranded coiled-coil domains of the human non-muscle myosin-IIA and myosin-IIB heavy chains were modeled using the crystal structure of the *Saccharomyces cerevisiae* Spc42p coiled coil (V. N. Malashkevich, unpublished results). The central part of the Spc42p coiled coil was extended to the desired length using O (*23*) and LSQKAB (*24*), and the structures of residues 1730−1928 of the myosin-IIA and myosin-IIB heavy chains were modeled using the threading algorithm from PDB VIEWER (*25*). The models were subjected to molecular dynamics using the simulated annealing protocol in CNS (*26*). Of several models with different initial velocities, those with the lowest free energy were selected for further analysis. The electrostatic potentials of the myosin-IIA and myosin-IIB rods were analyzed using PDB VIEWER and GRASP (*27*). The heptad repeat was identified using Paircoil (*28*).

Protein Purification. Recombinant human mts1 was purified as described previously (*29*). Recombinant human myosin-IIA rods and the GST−myosin-IIA fusion of residues 1900−1961 (GST−$MIIA_{1900-1961}$) were purified as described by Li et al. (*17*).

Chemical Cross-Linking of GST−$MIIA_{1900-1961}$. To examine the oligomeric state of the GST−myosin-IIA fusion, the bifunctional cross-linking reagent disuccinimidylsuberate (DSS) (Pierce) was added to final concentration of 10 mM to the GST−$MIIA_{1900-1961}$ or GST control in phosphate-buffered saline [0.137 M NaCl, 2.68 mM KCl, 0.01 M Na_2HPO_4, and 1.76 mM KH_2PO_4 (pH 7.5)]. The reaction mixtures were incubated for 1 h at room temperature and reactions stopped by the addition of Laemmli sample buffer (*30*) and heating. Parallel samples were incubated with dimethyl sulfoxide alone as a negative control. The untreated and cross-linked samples were subjected to SDS−PAGE and Coomassie-stained. DSS treatment of purified GST−$MIIA_{1900-1961}$ or GST alone resulted in the appearance of prominent bands at ~70 and ~55 kDa, which correspond to GST dimers (Figure 1). These observations indicate that GST−$MIIA_{1900-1961}$ does not form large oligomeric assemblies.

PKC and CK2 Phosphorylation of the Myosin-IIA Rods and GST−$MIIA_{1900-1961}$. The myosin-IIA rods or GST−$MIIA_{1900-1961}$ (15−30 μM dimers) were preincubated with 140 nM PKC α (Panvera) in a buffer containing 100 μg/mL phosphatidylserine, 20 μg/mL 1,2-dioleoyl-*sn*-glycerol (Avanti Polar Lipids), 20 mM Tris-HCl (pH 7.5), 200 mM NaCl, 0.5 mM DTT, 2 mM ATP, and a 1:250 dilution of phosphatase inhibitor cocktails I and II (Sigma Chemical Co.) at room temperature for 20 min. The phosphorylation reaction was initiated by the addition of $MgCl_2$ to a concentration of 5 mM and $CaCl_2$ to a concentration of 0.3 mM. Phosphorylation reactions were allowed to proceed for approximately 2 h at 30 °C with periodic mixing to prevent the myosin-IIA filaments from precipitating.

For CK2 phosphorylation, the myosin-IIA rods or GST−$MIIA_{1900-1961}$ (6−23 μM dimers) were incubated with 5000 units of CK2 (New England BioLabs) in 20 mM Tris-HCl (pH 7.5), 200 mM NaCl, 0.2 mM DTT, 0.5 mM ATP, 10 mM $MgCl_2$, and a 1:250 dilution of phosphatase inhibitor cocktails I and II, as described above, at 30 °C for 2 h.

To determine the extent of phosphate incorporation, parallel aliquots of the phosphorylation reaction were incubated with [γ-^{32}P]ATP. At different times, 4 μL of the reaction mixture was spotted onto 1 cm × 1 cm P81 phosphocellulose paper squares. The squares were washed extensively with 75 mM phosphoric acid and assessed for incorporation of ^{32}P using a Beckman LS scintillation counter. In addition, the extent of GST−$MIIA_{1900-1961}$ phosphorylation was monitored by glycerol−PAGE using the method of Perrie and Perry (*31*).

Following the phosphorylation reactions, PKC and CK2 were removed by successive cycles of assembly and disassembly of the myosin-IIA rods. An immunoblot with a PKCα/β antibody (Calbiochem) did not detect any remaining kinase in the cycled myosin-IIA. Phosphorylated, cycled myosin-IIA rods were used in assembly and mts1 binding assays.

Filament Assembly. Myosin-IIA rods (3 μM) were incubated overnight at 4 °C in 20 mM Tris-HCl (pH 7.5), 1 mM DTT, and 0.02% NaN_3 with varying concentrations of NaCl (from 0 to 500 mM) and 2 mM EDTA or 2 mM $MgCl_2$. The mixtures were centrifuged at 80 000 rpm (175000*g*) for 10 min at 25 °C in a TL-100 ultracentrifuge (Beckman). After ultracentrifugation, samples of the supernatants and pellets were separated on a 12% Tris-Tricine SDS−polyacrylamide gel, and the staining intensity of the myosin-IIA rods was compared with a standard curve of purified myosin-IIA rods run on the same gel. Wet gels were scanned, and the amount of polymerized myosin-IIA rods was quantified using ImageQuant version 5.0. The solubility data were plotted as a function of NaCl concentration and fit to the Hill equation to compare the steepness and midpoint of the curves for unphosphorylated and phosphorylated rods.

To examine the assembly properties of mixtures of PKC-phosphorylated and unphosphorylated myosin-IIA rods, 1:0, 1:1, 1:2, 1:4, and 0:1 molar ratios of PKC-phosphorylated to unphosphorylated myosin-IIA rods (total rod concentration of 3 μM) were evaluated in the sedimentation assay described above in the presence of 150 mM NaCl and 2 mM $MgCl_2$. The amount of myosin-IIA rod monomers recovered in the

supernatant was determined by densitometry of the Coomassie-stained gel. The distribution of PKC-phosphorylated protein was monitored by immunoblot analysis with a phosphoserine PKC substrate antibody (Cell Signaling) and quantified using ImageQuant version 5.0.

Cosedimentation Assays. For mts1−myosin-IIA rod binding assays, 3 μM (final concentration) unphosphorylated or phosphorylated myosin-IIA rods were incubated in a reaction mixture containing 0−200 μM mts1 dimer in 20 mM Tris-HCl (pH 7.5), 20 mM NaCl, 2 mM $MgCl_2$, 0.3 mM $CaCl_2$, 1 mM DTT, and 0.02% NaN_3 for 1 h at room temperature. The mixtures were centrifuged at 80 000 rpm (175000*g*) for 10 min at 25 °C in a TL-100 ultracentrifuge (Beckman). Samples of supernatants and pellets were separated on a 12% Tris-Tricine SDS−polyacrylamide gel. Wet gels were scanned and quantified using ImageQuant version 5.0. The staining intensity of mts1 was compared with a standard curve of purified recombinant human mts1 run on the same gel. The equilibrium binding constant was estimated by a nonlinear least-squares fit using an equation which takes into account ligand depletion $\{MR = 0.5(K_d + R_{tot} + M_{tot}) \pm [-(K_d + R_{tot} + M_{tot})^2 - 4M_{tot}R_{tot}]^{1/2}$, where MR is the mts1·myosin-II complex concentration, R_{tot} is the total myosin-II concentration, and M_{tot} is the total mts1 concentration (*32*)}.

Glutathione Bead Pelleting Assay. Unphosphorylated or phosphorylated GST−$MIIA_{1900-1961}$ (3 μM) or control GST (3 μM) was bound to glutathione−Sepharose and incubated with 0−40 μM mts1 dimer in 20 mM Tris-HCl (pH 7.5), 50 mM NaCl, 2 mM $MgCl_2$, 0.3 mM $CaCl_2$, 0.5 mM DTT, 0.02% NaN_3, and 0.5 mg/mL BSA for 1 h at room temperature. The mixtures were centrifuged at 5000*g* for 2 min and the supernatants removed. The glutathione−Sepharose pellets were washed five times with binding buffer, resuspended in Laemmli sample buffer (*30*), and analyzed on a 12% Tris-Tricine SDS−PAGE gel. Wet gels were scanned and quantified using ImageQuant version 5.0 as described above.

Inhibition of Filament Assembly by Mts1. Unphosphorylated or phosphorylated monomeric myosin-IIA rods (3 μM) were added to a reaction mixture containing 0−36 μM mts1 dimer in 20 mM Tris-HCl (pH 7.5), 300 mM NaCl, 2 mM $MgCl_2$, 0.3 mM $CaCl_2$, 1 mM DTT, and 0.02% NaN_3 and incubated for 15 min at room temperature. An aliquot of the mix was removed for SDS−PAGE, and the remaining reaction mixture was diluted to yield final concentrations of 1.5 μM myosin-IIA rods, 0−18 μM mts1 dimer, and 150 mM NaCl as described previously (*17*). The reaction mixtures were incubated for 1 h at room temperature and centrifuged at 80 000 rpm for 10 min at 25 °C in a TL-100 ultracentrifuge (Beckman). Samples of the supernatants and pellets were separated on a 12% Tris-Tricine SDS−polyacrylamide gel, and the amount of protein recovered in the supernatants was determined by densitometry as described above and quantified using ImageQuant version 5.0.

Promotion of Filament Disassembly by Mts1. Assembled myosin-IIA rods (3 μM) were added to a reaction mixture containing 0−36 μM mts1 dimer in 20 mM Tris-HCl (pH 7.5), 150 mM NaCl, 2 mM $MgCl_2$, 0.3 mM $CaCl_2$, 1 mM DTT, and 0.02% NaN_3 for 1 h at room temperature. A sample of the mix was taken for SDS−PAGE analysis, and the remaining mixtures were centrifuged as described above. Samples of the supernatants and pellets were separated on a 12% Tris-Tricine SDS−polyacrylamide gel, and the amount of protein recovered in the supernatants was determined by densitometry as described above and quantified using ImageQuant version 5.0.

RESULTS

Molecular Modeling of the ACD and Extended ACD. To examine the mechanisms that may contribute to the regulation of myosin-IIA assembly, a model was constructed of residues 1730−1928, which encompasses the extended ACD (residues 1858−1920) from the C-terminal end of the α-helical coiled coil (Figure 2A−C). Despite the fact that the myosin-II rod is predicted to form a two-stranded coiled coil, there are several factors that can significantly reduce the stability of the coiled coil. Kwok and Hodges (*33*) demonstrated that clusters of three or more Leu, Ile, Val, Met, Phe, or Tyr residues in the *a* and *d* positions of the heptad repeat stabilize coiled coils, whereas clusters of other amino acids destabilize coiled-coil structures. Within the ACD, a cluster of three stabilizing residues (Leu1873, Leu1876, and Leu1880) is followed by a cluster of four destabilizing residues (Ala1883, Ala1887, Ala1890, and Arg1894) (Figure 2A,B), suggesting that this region of the coiled coil is flexible, consistent with its proposed role in regulating filament assembly. On the basis of the observations that native and in vitro myosin filaments display an approximately 14 nm axial shift and that the rod exhibits a striking pattern of alternating charged residues, electrostatic interactions are thought to mediate parallel and antiparallel alignment of myosin-II monomers during filament assembly (*34*−*37*). The electrostatic potential features within the modeled sequences of myosin-IIA and myosin-IIB (Figure 2C,D) are notably alike, suggesting similar assembly mechanisms. However, the mts1 binding site in myosin-IIA has more negative potential, which may account for the differential effects of mts1 binding on myosin-IIA and myosin-IIB assembly and disassembly (*17*). In addition, we noted that the PKC phosphorylation site (S1917) is adjacent to a region that contains a large number of basic residues.

Phosphorylation of the Myosin-IIA Heavy Chain. We established conditions for stoichiometric phosphorylation of the myosin-IIA rods with either PKC or CK2. PKC incorporated 2.1 mol of phosphate per mole of myosin-IIA rods (1.0 mol of phosphate per myosin heavy chain polypeptide) (Figure 3A). For CK2, the final extent of phosphate incorporation was 2.2 mol of phosphate per mole of myosin-IIA rods (1.1 mol of phosphate per myosin heavy chain polypeptide) (Figure 3B). These stoichiometries are consistent with Ser1917 and Ser1944 being the sole sites of PKC and CK2 phosphorylation on the myosin-IIA heavy chain, respectively (*14*, *15*, *38*).

Effects of Heavy Chain Phosphorylation on Myosin-IIA Filament Assembly. Previous studies demonstrated that phosphorylation by PKC or CK2 strongly inhibited the assembly of myosin-IIB, but not myosin-IIA (*13*, *16*). However, since these studies did not utilize stoichiometrically phosphorylated myosin-IIA, we decided to re-examine the effects of heavy chain phosphorylation on myosin-IIA filament formation with a myosin-IIA rod construct that we previously demonstrated to be assembly competent (*17*). Our current studies indicate that phosphorylation of the heavy

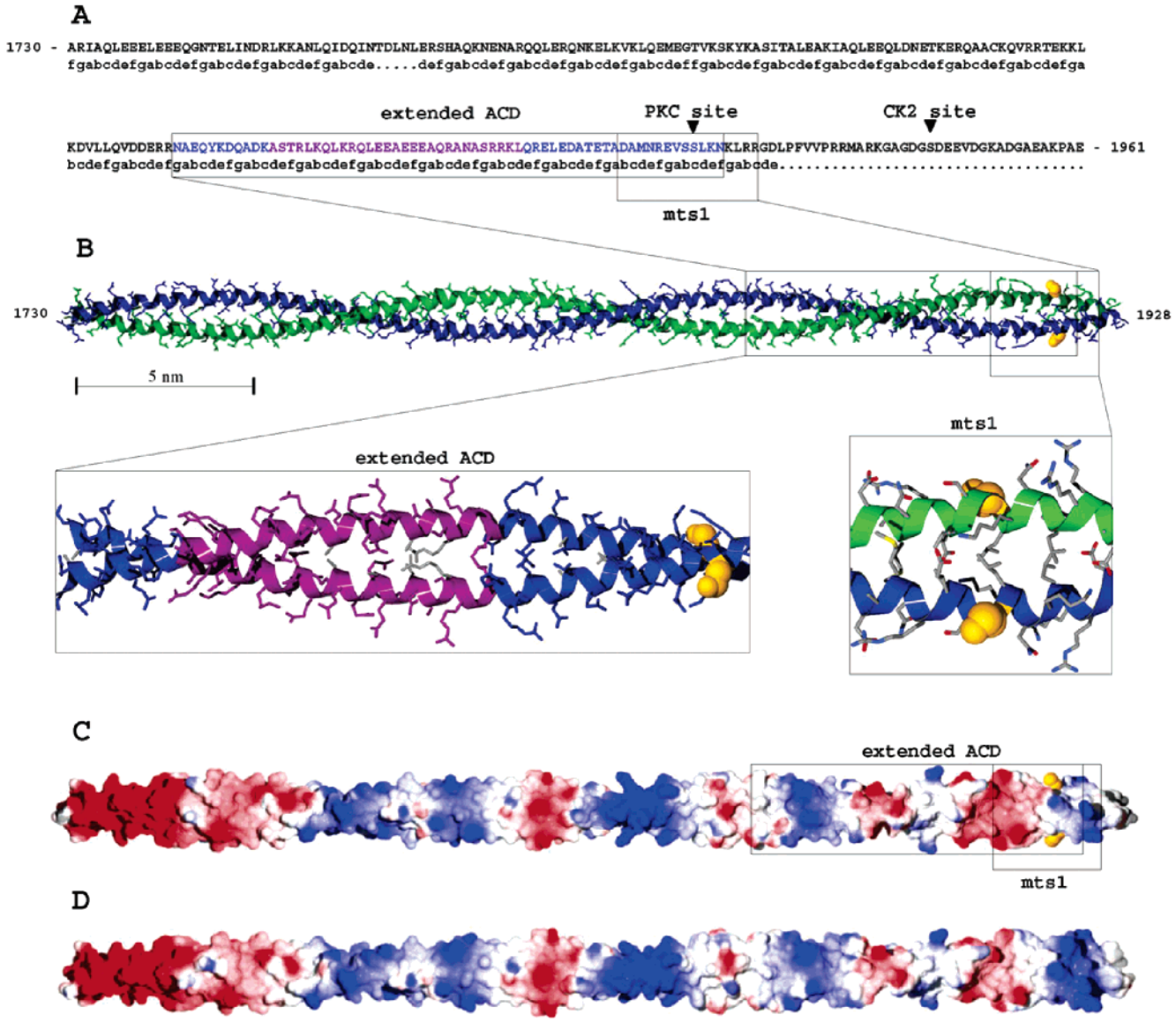

FIGURE 2: Molecular model of the myosin-IIA α-helical coiled coil. (A) Residues 1730−1961 of the myosin-IIA heavy chain sequence with the heptad repeat shown below the sequence. Two areas of interest are framed and magnified within the molecular model in panel B: the ACD (residues 1869−1897 in purple) and the extended ACD (residues 1858−1920 in blue), and the mts1 binding site (residues 1909−1924). The PKC phosphorylation site at Ser1917 and the CK2 phosphorylation site at Ser1944 are depicted with arrows. (B) Molecular model of residues 1730−1928 from the coiled coil. The PKC phosphorylation site at Ser1917 is colored gold. The ACD and the extended ACD (left magnified window) are highlighted in purple and blue, respectively. This area contains nine destabilizing residues (gray) in the *a* and *d* positions of the heptad repeat. The PKC phosphorylation site and the mts1 binding site (right magnified window) are adjacent to an area of relatively negative electrostatic potential. (C) Molecular surface presentation of the electrostatic potential of residues 1730−1928 of the myosin-IIA α-helical coiled coil. Blue and red represent regions of positive and negative potential, respectively (±3 kT/e$^-$ range). (D) Molecular surface presentation of the electrostatic potential of residues 1730−1928 of the myosin-IIB α-helical coiled coil. Note the relatively more negative potential within the mts1 binding area of myosin-IIA.

chain by either PKC or CK2 significantly inhibits filament formation. At pH 7.5 in the presence of 2 mM $MgCl_2$ and 150 mM NaCl (physiological salt concentration), approximately 85% of the unphosphorylated myosin-IIA rods were assembled. In contrast, only 40 and 35% of the PKC- and CK2-phosphorylated rods, respectively, assembled under identical conditions (Figure 4A). Furthermore, at salt concentrations below 50 mM NaCl, greater than 90% of the unphosphorylated and CK2-phosphorylated myosin-IIA rods assembled, whereas only 60% of the PKC-phosphorylated rods formed filaments, demonstrating that PKC phosphorylation impaired the assembly of the myosin-IIA rods. When assembly was performed in the absence of $MgCl_2$, both the unphosphorylated and phosphorylated rods displayed increased solubility, with only 60% of the unphosphorylated and 25% of the PKC- and 25% of the CK2-phosphorylated rods forming filaments in the presence of 150 mM NaCl (Figure 4B). An examination of the Hill coefficients indicates that in the presence and absence of magnesium, heavy chain phosphorylation significantly affects the steepness of the curve with PKC phosphorylation having a more pronounced effect than CK2 phosphorylation (Table 1). In addition, a comparison of the midpoints shows that in the presence of magnesium the assembly of CK2-phosphorylated rods is more sensitive to the NaCl concentration than unphosphorylated and PKC-phosphorylated myosin-IIA rods.

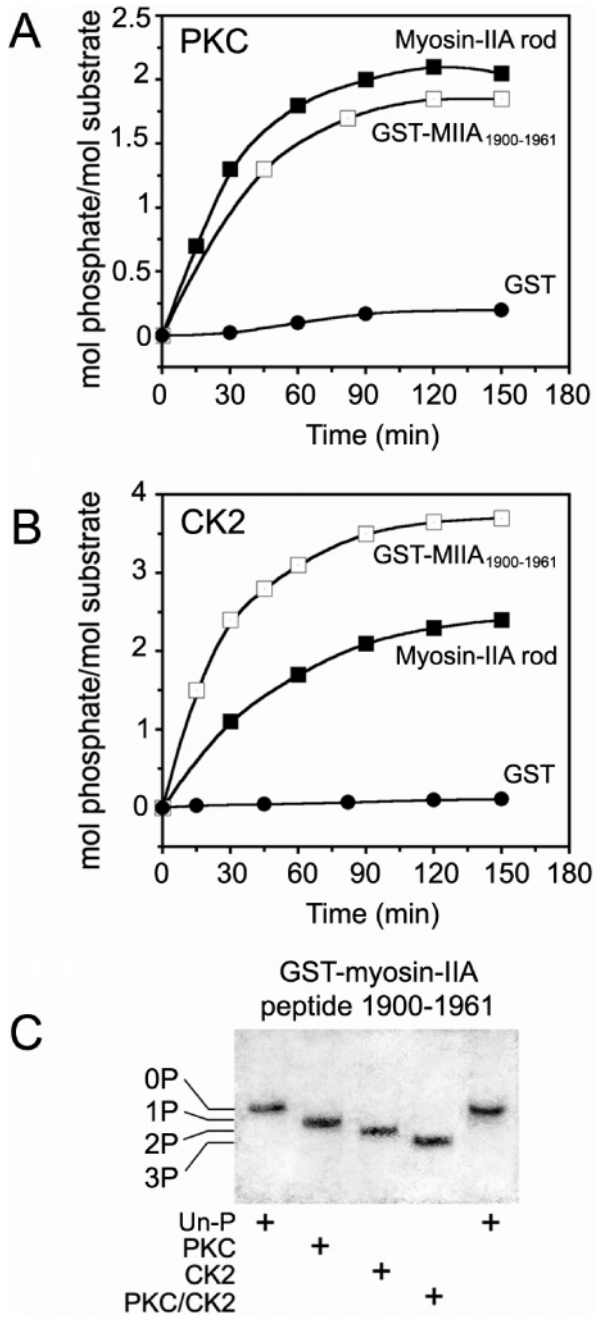

FIGURE 3: Time course of phosphorylation of the myosin-IIA rods and GST−$MIIA_{1900-1961}$ with PKC or CK2. (A) PKC phosphorylation or (B) CK2 phosphorylation of the myosin-IIA rods and GST−$MIIA_{1900-1961}$ was monitored using [γ-^{32}P]ATP as described in Experimental Procedures: (■) myosin-IIA rods, (□) GST−$MIIA_{1900-1961}$, and (●) GST. (C) Glycerol−PAGE and Coomassie staining of GST−$MIIA_{1900-1961}$ phosphorylated with PKC or CK2. Incorporation of phosphate groups increases the electrophoretic mobility of the GST−myosin-IIA fusion on a glycerol gel. Marks indicate the mobility of the GST fusion with zero, one, two, or three phosphates.

Next, we examined the effect of unphosphorylated rods on the assembly of PKC-phosphorylated rods at physiological salt concentrations in the presence of magnesium. Stoichiometrically phosphorylated myosin-IIA rods were mixed with unphosphorylated myosin-IIA rods at varying molar ratios, and the percent recovery of the myosin-IIA fragments in the supernatant after assembly was determined (Figure 5). Immunoblot analysis with a phosphoserine antibody revealed that a molar excess of unphosphorylated rods does not influence the assembly of PKC-phosphorylated rods since ~70% of the PKC-phosphorylated rods were recovered in the supernatants regardless of the amount of unphosphorylated rods in the assembly reaction mixture (Figure 5B). The presence of PKC-phosphorylated rods did not affect the assembly of the unphosphorylated rods as ~20% of the unphosphorylated rods were detected in the supernatant under all conditions that were examined. These observations indicate that PKC-phosphorylated and unphosphorylated myosin-IIA rods assemble independently of one another under these experimental conditions.

Binding of Mts1 to Phosphorylated Myosin-IIA. Previous studies showed that a molar excess of mts1 inhibits both PKC and CK2 phosphorylation of the myosin-IIA heavy chain (*21*, *22*). To evaluate if heavy chain phosphorylation affects the equilibrium binding of mts1, we utilized a GST fusion containing residues 1900−1961 of the human myosin-IIA heavy chain, which we showed previously contains the mts1 binding site (*17*). PKC incorporated 1.8 mol of phosphate per mole of GST−$MIIA_{1900-1961}$ dimer (0.9 mol of phosphate per myosin heavy chain polypeptide), and CK2 incorporated 3.6 mol of phosphate per mole of GST−$MIIA_{1900-1961}$ dimer (1.8 mol of phosphate per myosin heavy chain polypeptide) (Figure 3A,B). No phosphate incorporation was detected for GST alone by either kinase. In addition, we found that the extent of GST−$MIIA_{1900-1961}$ phosphorylation could be monitored by glycerol−polyacrylamide gel electrophoresis (Figure 3C). Phosphate incorporation increased the electrophoretic mobility of GST−$MIIA_{1900-1961}$ in a manner similar to that observed for the regulatory light chain of myosin-II (*31*). The incorporation of up to three phosphate groups could be easily distinguished using this gel electrophoresis system.

Using a quantitative glutathione−Sepharose pull-down assay, we observed that CK2 phosphorylation inhibited the equilibrium binding of mts1 to the myosin-IIA heavy chain, as compared to unphosphorylated GST−$MIIA_{1900-1961}$ and PKC-phosphorylated GST−$MIIA_{1900-1961}$ (Figure 6). The equilibrium dissociation constant for the binding of mts1 to unphosphorylated GST−$MIIA_{1900-1961}$ and PKC-phosphorylated GST−$MIIA_{1900-1961}$ could not be determined as these binding curves could not be distinguished from a stoichiometric titration of the GST−myosin-IIA fusion and mts1; however, we were able to determine an approximate K_d of 4.78 ± 2.86 μM for the binding of mts1 to CK2-phosphorylated GST−$MIIA_{1900-1961}$. When GST−$MIIA_{1900-1961}$ was phosphorylated by both PKC and CK2, mts1 had the same affinity for the myosin-IIA heavy chain as for just the CK2-phosphorylated material, indicating that only CK2 phosphorylation regulates the interaction of mts1 with the myosin-IIA heavy chain and that the effects of PKC and CK2 phosphorylation are not coupled. The stoichiometry of binding was not affected by heavy chain phosphorylation as mts1 bound to unphosphorylated and PKC-, CK2-, and PKC/CK2-phosphorylated GST−$MIIA_{1900-1961}$ with stoichiometries of approximately 1 mol of mts1 dimer per mole of myosin-IIA peptide.

To confirm and extend this analysis, we evaluated the equilibrium binding of mts1 to unphosphorylated and PKC- and CK2-phosphorylated myosin-IIA rods in a cosedimentation assay (Figure 7 and Table 2). These binding studies

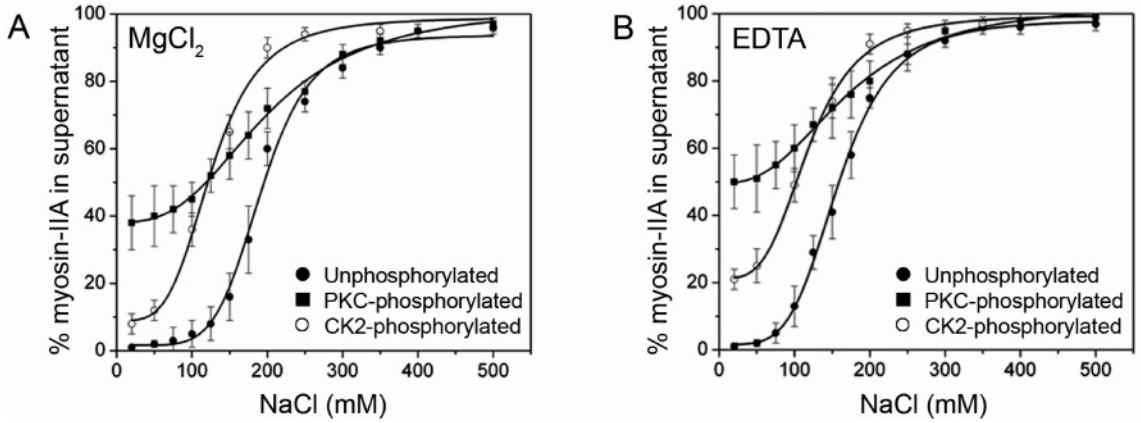

FIGURE 4: Assembly properties of PKC- and CK2-phosphorylated myosin-IIA rods. The assembly of unphosphorylated and phosphorylated myosin-IIA rods (3 μM) was monitored using a standard sedimentation assay. Assembly in the presence of (A) $MgCl_2$ or (B) EDTA: (●) unphosphorylated myosin-IIA rods, (■) PKC-phosphorylated myosin-IIA rods, and (○) CK2-phosphorylated myosin-IIA rods. Values represent the mean and the standard deviation of the mean for three to five independent experiments. The solid lines represent the best fit to the Hill equation.

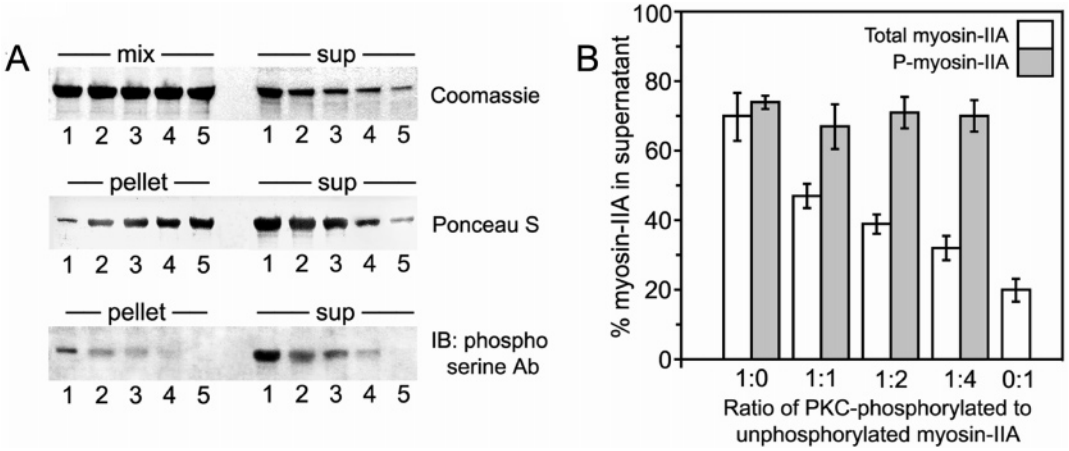

FIGURE 5: Co-assembly of unphosphorylated and PKC-phosphorylated myosin-IIA rods. The effect of PKC-phosphorylated rods on the assembly of unphosphorylated rods was examined in a sedimentation assay. (A, top) Coomassie-stained SDS−polyacrylamide gel showing mixes and supernatants from the assembly assay: lane 1, 3 μM PKC-phosphorylated myosin-IIA rods; lanes 2−4, 1:1, 1:2, and 1:4 molar ratios of PKC-phosphorylated to unphosphorylated myosin-IIA rods (total rod concentration of 3 μM), respectively; and lane 5, 3 μM unphosphorylated myosin-IIA rods. (Middle) Ponceau S-stained nitrocellulose showing pellets and supernatants from the assembly assay. (Bottom) Immunoblot analysis of pellets and supernatants from the assembly assay with a phosphoserine antibody to monitor the distribution of the PKC-phosphorylated myosin-IIA rods. (B) The amount of myosin-IIA monomers recovered in the supernatant was determined by densitometry of the Coomassie gel and shown in panel A. Values represent the mean and the standard deviation of the mean for three independent experiments.

Table 1: Summary of the Dependence of Myosin-IIA Rod Assembly on the Sodium Concentration[a]

myosin-IIA rods	n_H	midpoint (mM)
$MgCl_2$		
unphosphorylated	5.9 ± 0.5	192.3 ± 2.9
PKC-phosphorylated	2.8 ± 0.4	199.5 ± 11.1
CK2-phosphorylated	3.9 ± 0.4	126.4 ± 3.8
EDTA		
unphosphorylated	4.4 ± 0.2	159.1 ± 1.5
PKC-phosphorylated	2.6 ± 0.2	173.1 ± 6.1
CK2-phosphorylated	3.6 ± 0.3	119.4 ± 2.5

[a] Values represent the mean and the standard deviation of the mean for three to five independent experiments.

were performed at a low ionic strength (i.e., 20 mM NaCl), which are conditions that enhance the stability of the myosin-II filaments and will prevent their disassembly by mts1 (*17*). As in our binding studies utilizing GST−$MIIA_{1900-1961}$, we observed that CK2 phosphorylation decreased the affinity of mts1 for the myosin-IIA heavy chain (~6.5-fold) as compared to unphosphorylated and PKC-phosphorylated myosin-IIA rods. The stoichiometry of binding to unphosphorylated and PKC- and CK2-phosphorylated rods was 0.38, 0.72, and 0.26 mol of mts1 dimer per mole of dimeric myosin-II rod, respectively. Similar binding stoichiometries were observed for CK2-phosphorylated and unphosphorylated filaments (*17*), whereas enhanced binding was detected for PKC-phosphorylated filaments. This increase likely occurs due to the reduced assembly properties of PKC-phosphorylated filaments and may reflect looser packing of PKC-phosphorylated filaments.

Effects of Heavy Chain Phosphorylation on Mts1-Mediated Regulation of the Myosin-II Monomer−Polymer Equilibrium. Next we examined the role of heavy chain phosphorylation in modulating mts1-mediated inhibition of filament assembly at physiological salt concentrations. In the absence of mts1, ~45% of the PKC- and CK2-phosphorylated myosin-IIA rods were present in the supernatant (Figures 8 and 9), consistent with our observation that heavy chain phospho-

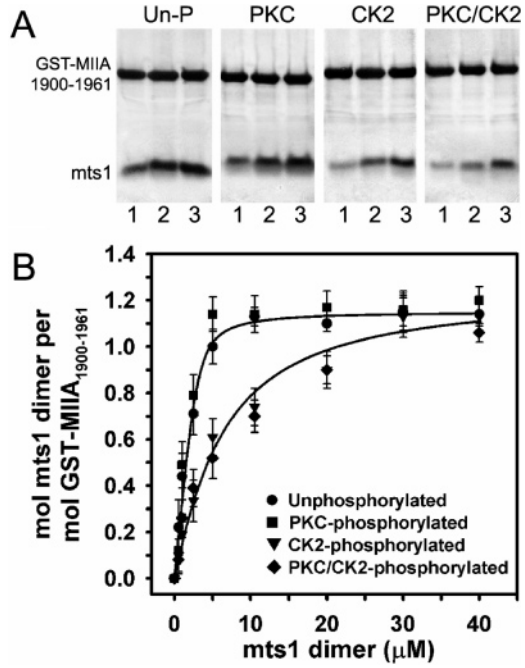

FIGURE 6: Binding of mts1 to phosphorylated GST−$MIIA_{1900-1961}$. A glutathione bead copelleting assay was performed using unphosphorylated and PKC- and CK2-phosphorylated GST−$MIIA_{1900-1961}$. (A) A Coomassie-stained SDS−polyacrylamide gel showing samples of GST−$MIIA_{1900-1961}$ immobilized on glutathione−Sepharose and bound mts1. Assays were performed using a pH 7.5 buffer containing 50 mM NaCl, 2 mM $MgCl_2$, and 0.3 mM $CaCl_2$. Lanes 1−3 are assays utilizing 1, 2.5, and 5 μM mts1 dimer in the incubation mixture, respectively. (B) The amount of mts1 dimer bound per mole of GST−$MIIA_{1900-1961}$ was determined for each mts1 concentration. Values represent the mean and the standard deviation of the mean for three independent experiments. The solid lines represent the best fit to the quadratic equation that considers ligand depletion.

rylation partially impedes filament formation (Figure 4). The addition of mts1 further inhibited the assembly of PKC-phosphorylated rods. At a molar ratio of 1 mts1 dimer per myosin-IIA rod, we observed maximal inhibition of assembly with ~80% of the PKC-phosphorylated myosin-IIA remaining in the supernatant (Figure 8A), which is identical to mts1-mediated effects on the assembly of unphosphorylated rods (*17*). In contrast, mts1 had only a minor effect on the assembly of CK2-phosphorylated filaments with ~55% of the rods present in the supernatant at a molar ratio of 1 mts1 dimer per myosin-IIA rod (Figure 8B). We also assessed whether heavy chain phosphorylation had any effect on the destabilization of myosin-IIA filaments by mts1. At a molar ratio of 1 mts1 dimer per myosin-IIA rod, we observed maximal disassembly of PKC-phosphorylated filaments with ~90% of the myosin-IIA in the supernatant (Figure 9A), which is comparable to the extent of disassembly observed for unphosphorylated filaments (*17*). Disassembly of CK2-phosphorylated filaments was modest with only ~55% of the rods present in the supernatant at a molar ratio of 1 mts1 dimer per myosin-IIA rod (Figure 9B). These biochemical studies demonstrate that CK2 phosphorylation protects against mts1-induced inhibition of filament assembly and mts1-induced destabilization of myosin II filaments, and also suggest that phosphorylation on the CK2 site of the myosin-IIA heavy chain may provide an additional level of regulation for the mts1−myosin-IIA interaction in vivo.

DISCUSSION

The assembly of non-muscle myosin-II is regulated by phosphorylation on the regulatory light chain (*39*), as well as by phosphorylation on the heavy chain (*13*, *16*). Previous studies utilizing myosin-II rod fragments provided evidence that PKC and CK2 phosphorylation on the heavy chain regulates filament assembly of vertebrate myosin-II and that this effect is isoform-specific. Phosphorylation by either PKC or CK2 was reported to strongly inhibit the assembly of myosin-IIB, whereas it did not obviously affect myosin-IIA filament formation (*13*, *16*). Our studies, which utilized a longer myosin-IIA rod fragment, demonstrate for the first time that phosphorylation of the myosin-IIA heavy chain significantly inhibits filament formation. This discrepancy is likely a consequence of the substoichiometric level of phosphate incorporation onto the myosin-IIA heavy chain in earlier studies with 0.5 and 0.75 mol of phosphate per myosin heavy chain polypeptide for PKC and CK2, respectively (*13*), as compared to 1.0 mol of phosphate per myosin heavy chain polypeptide for PKC and 1.1 mol of phosphate per myosin heavy chain polypeptide for CK2 in this study. Thus, it appears that the extent of inhibition of myosin-IIA assembly depends on the level of incorporation of phosphate into the PKC and CK2 sites. This is consistent with our observation that at substoichiometric levels of phosphate incorporation, myosin-IIA filament formation was affected to a lesser extent than for stoichiometrically phosphorylated myosin-IIA (unpublished observations). Our findings that inhibition of myosin-IIA assembly requires stoichiometric

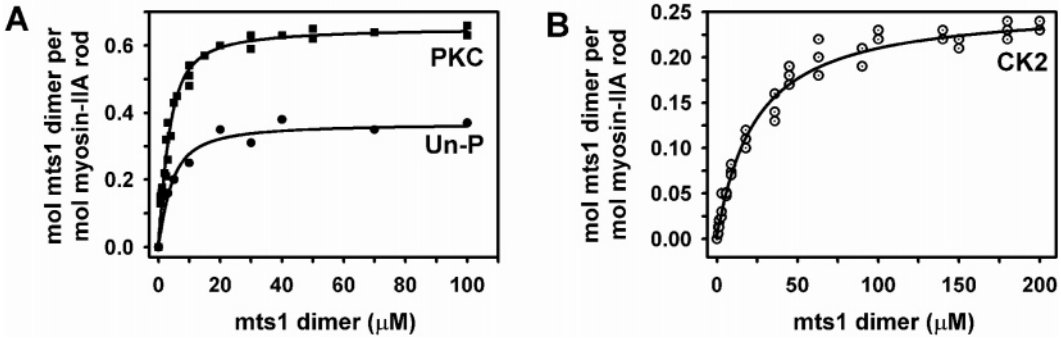

FIGURE 7: Binding of mts1 to phosphorylated myosin-IIA rods. Mts1 was cosedimented with unphosphorylated and PKC- and CK2-phosphorylated myosin-IIA rods in 20 mM NaCl, 2 mM $MgCl_2$, and 0.3 mM $CaCl_2$ (pH 7.5). The number of moles of mts1 dimer bound per mole of myosin-IIA rod was determined for each mts1 concentration. The solid lines represent the best fit to the quadratic equation that considers ligand depletion.

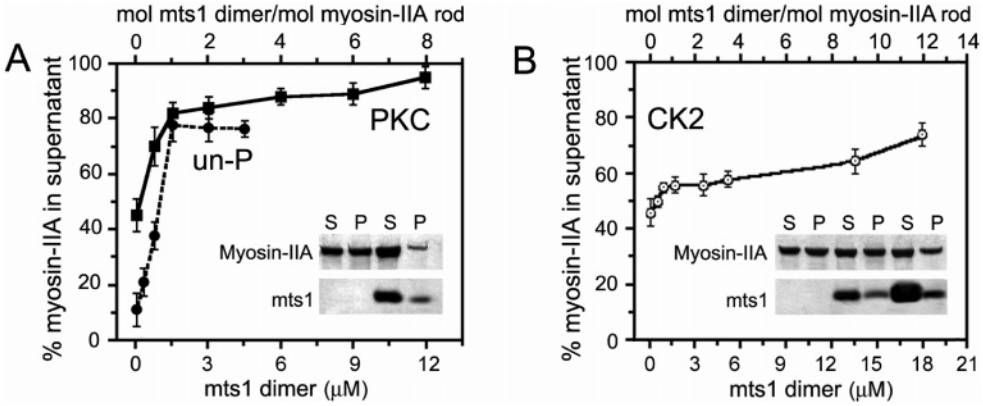

FIGURE 8: CK2 phosphorylation protects against mts1-mediated inhibition of myosin-IIA assembly. Assays were performed using a pH 7.5 buffer containing 150 mM NaCl, 2 mM $MgCl_2$, and 0.3 mM $CaCl_2$. (A) At 1 mol of mts1 dimer per mole of myosin-IIA rod, mts1 strongly inhibits the assembly of PKC-phosphorylated myosin-IIA monomers in a manner similar to that of unphosphorylated rods. The inset shows SDS−PAGE of PKC-phosphorylated myosin-IIA assembly monitored in a standard pelleting assay. In the absence of mts1, ~45% of the myosin-IIA rods are recovered in the supernatant (lanes 1 and 2). At a molar ratio of 8 mts1 dimers per myosin-IIA rod, ~94% of the myosin-IIA rods are recovered in the supernatant (lanes 3 and 4). (B) Mts1 had only a modest effect on the assembly of CK2-phosphorylated myosin-IIA monomers. The inset shows SDS−PAGE of CK2-phosphorylated myosin-IIA assembly monitored in a standard pelleting assay. In the absence of mts1, ~45% of the myosin-IIA rods are recovered in the supernatant (lanes 1 and 2). At a molar ratio of 9 mts1 dimers per myosin-IIA rod, ~63% of the myosin-IIA rods are recovered in the supernatant (lanes 3 and 4). Values represent the mean and standard deviation of the mean for three independent experiments.

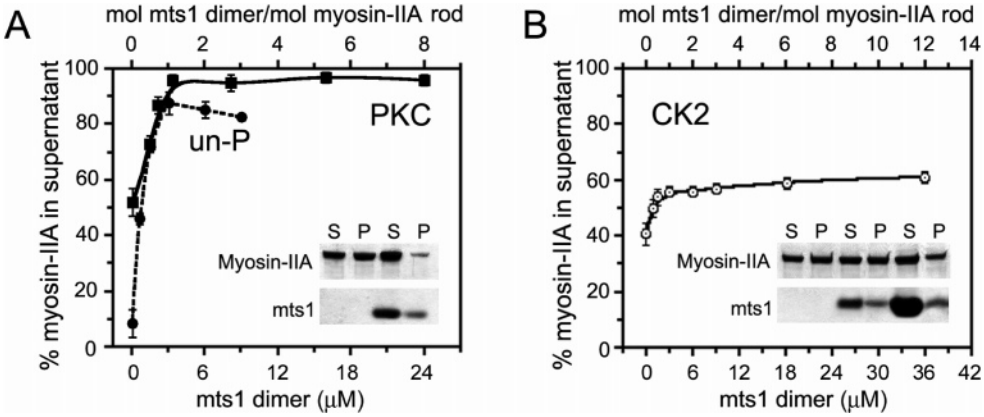

FIGURE 9: CK2 phosphorylation inhibits mts1-mediated disassembly of myosin-IIA filaments. Assays were performed using a pH 7.5 buffer containing 150 mM NaCl, 2 mM $MgCl_2$, and 0.3 mM $CaCl_2$. (A) For PKC-phosphorylated myosin-IIA rods, maximal promotion of disassembly was observed at 1 mol of mts1 dimer per mole of myosin-IIA rod, as for unphosphorylated rods. The inset shows SDS−PAGE of PKC-phosphorylated myosin-IIA disassembly monitored in a standard pelleting assay. In the absence of mts1, ~50% of the myosin-IIA rods are recovered in the supernatant (lanes 1 and 2). At a molar ratio of 5 mts1 dimers per myosin-IIA rod, ~96% of the myosin-IIA rods are recovered in the supernatant (lanes 3 and 4). (B) Mts1 had only a modest effect on the stability of CK2-phosphorylated myosin-IIA filaments. The inset shows SDS−PAGE of CK2-phosphorylated myosin-IIA disassembly monitored in a standard pelleting assay. In the absence of mts1, ~40% of the myosin-IIA rods are recovered in the supernatant (lanes 1 and 2). At a molar ratio of 6 mts1 dimers per myosin-IIA rod, ~58% of the myosin-IIA rods are recovered in the supernatant (lanes 3 and 4). Values represent the mean and standard deviation of the mean for three independent experiments.

Table 2: Effect of Heavy Chain Phosphorylation on Mts1 Binding[a]

myosin-IIA rods	K_d (μM)
unphosphorylated	2.62 ± 1.41
PKC-phosphorylated	1.77 ± 0.91
CK2-phosphorylated	21.86 ± 4.40

[a] Values represent the mean and the standard deviation of the mean for three to six independent experiments.

phosphorylation, and that assembly of phosphorylated and unphosphorylated rods is independent, suggest that heavy chain phosphorylation may allow for localized control of filament assembly in vivo and provides a mechanism by which the cell can fine-tune filament formation depending on local cellular needs.

In addition to regulating assembly, we provide the first quantitative evidence that heavy chain phosphorylation also modulates mts1 binding. Despite the fact that the mts1 binding site overlaps the PKC phosphorylation site on the myosin-IIA heavy chain, mts1 binding is not affected by PKC phosphorylation. Consistent with this observation, mts1 inhibition of myosin-IIA assembly and mts1-mediated disassembly of preformed filaments was identical for unphosphorylated and PKC-phosphorylated rods. Since structural studies have shown that hydrophobic interactions largely mediate the binding of S100 family proteins to single helical peptides (*40*−*42*), we propose that the two chains of the myosin-IIA coiled coil must "unzip" to provide the appropriate nonpolar binding interface for mts1 and that Ser1917, the PKC phosphorylation site, is located on the face of the myosin-IIA helix opposite the mts1 binding site. The previous observation that mts1 binding inhibits PKC phosphorylation likely reflects the relative inaccessibility of

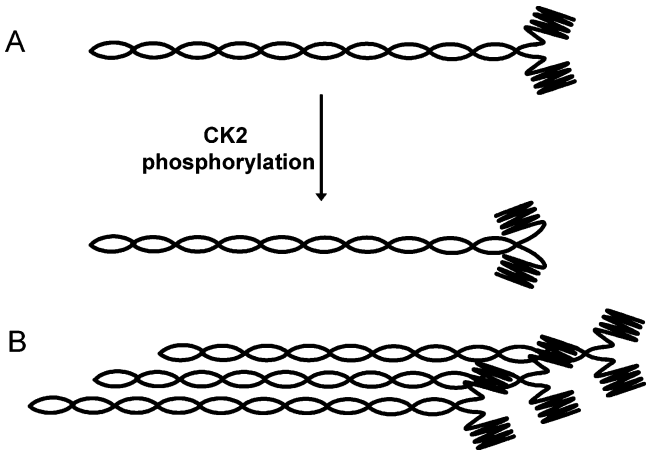

FIGURE 10: Models for inhibition of mts1 binding by CK2 phosphorylation on the myosin-IIA heavy chain. (A) CK2 phosphorylation induces a conformational change that allows the tailpiece to fold back and interfere with mts1 binding through interactions between the tailpiece and the helical rod. (B) Intermolecular interactions between adjacent monomers regulate mts1 binding.

Ser1917 to PKC due to steric interference when mts1 is bound to the myosin-IIA rod.

To our surprise, phosphorylation on the CK2 site, which is located 20 residues downstream of the mts1 binding site in the tailpiece, inhibits mts1 binding. Moreover, CK2 phosphorylation protects against mts1-induced inhibition of filament assembly and mts1-induced destabilization of myosin-IIA filaments. We envision two possible mechanisms by which phosphorylation on the CK2 site could modulate mts1 binding (Figure 10). In the first model, inhibition of mts1 binding occurs due to molecular interactions within a single myosin-IIA monomer. Phosphorylation induces a conformational change in the tailpiece that either is transmitted to the C-terminal end of the coiled coil to inhibit mts1 binding or allows the tailpiece to fold back and interfere with mts1 binding via intramolecular interactions between the tailpiece and helical rod. Our observation that mts1 displays a reduced affinity for CK2-phosphorylated GST−MIIA$_{1900-1961}$, which is a single polypeptide chain, indicates that intramolecular interactions can, in part, modulate mts1 binding. In the second model, intermolecular interactions between adjacent myosin-II monomers would regulate mts1 binding. Electron micrographs have shown that nonsarcomeric myosin-II molecules pack with an 14 nm parallel stagger relative to one another and also interact with an antiparallel partner via an ~14 nm overlap at the tip of the tail (*43*). These observations suggest that the tailpiece on one myosin-II monomer can interact with the C-terminal end of the coiled coil of the adjacent parallel monomer as well as with the C-terminus of the antiparallel partner. Thus, conformational changes that occur in the tailpiece upon phosphorylation could mediate mts1 binding on adjacent monomers.

ACKNOWLEDGMENT

We thank Dr. Michael Brenowitz and Mr. Dukagjin Blakaj for helpful discussions and assistance with data analysis.

REFERENCES

1. Saez, C. G., Myers, J. C., Shows, T. B., and Leinwand, L. A. (1990) Human nonmuscle myosin heavy chain mRNA: Generation of diversity through alternative polyadenylylation, *Proc. Natl. Acad. Sci. U.S.A. 87*, 1164−1168.
2. Simons, M., Wang, M., McBride, O. W., Kawamoto, S., Yamakawa, K., Gdula, D., Adelstein, R. S., and Weir, L. (1991) Human nonmuscle myosin heavy chains are encoded by two genes located on different chromosomes, *Circ. Res. 69*, 530−539.
3. Phillips, C. L., Yamakawa, K., and Adelstein, R. S. (1995) Cloning of the cDNA encoding human nonmuscle myosin heavy chain-B and analysis of human tissues with isoform-specific antibodies, *J. Muscle Res. Cell Motil. 16*, 379−389.
4. Golomb, E., Ma, X., Jana, S. S., Preston, Y. A., Kawamoto, S., Shoham, N. G., Goldin, E., Conti, M. A., Sellers, J. R., and Adelstein, R. S. (2004) Identification and characterization of nonmuscle myosin II-C, a new member of the myosin II family, *J. Biol. Chem. 279*, 2800−2808.
5. Maupin, P., Phillips, C. L., Adelstein, R. S., and Pollard, T. D. (1994) Differential localization of myosin-II isozymes in human cultured cells and blood cells, *J. Cell Sci. 107*, 3077−3090.
6. Itoh, K., and Adelstein, R. S. (1995) Neuronal cell expression of inserted isoforms of vertebrate nonmuscle myosin heavy chain II-B, *J. Biol. Chem. 270*, 14533−14540.
7. Kolega, J. (1998) Cytoplasmic dynamics of myosin IIA and IIB: Spatial 'sorting' of isoforms in locomoting cells, *J. Cell Sci. 111*, 2085−2095.
8. Rosenfeld, S. S., Xing, J., Chen, L. Q., and Sweeney, H. L. (2003) Myosin IIb is unconventionally conventional, *J. Biol. Chem. 278*, 27449−27455.
9. Wang, F., Kovacs, M., Hu, A., Limouze, J., Harvey, E. V., and Sellers, J. R. (2003) Kinetic mechanism of non-muscle myosin IIB: Functional adaptations for tension generation and maintenance, *J. Biol. Chem. 278*, 27439−27448.
10. Kovacs, M., Wang, F., Hu, A., Zhang, Y., and Sellers, J. R. (2003) Functional divergence of human cytoplasmic myosin II: Kinetic characterization of the non-muscle IIA isoform, *J. Biol. Chem. 278*, 38132−38140.
11. Sellers, J. R., Pato, M. D., and Adelstein, R. S. (1981) Reversible phosphorylation of smooth muscle myosin, heavy meromyosin, and platelet myosin, *J. Biol. Chem. 256*, 13137−13142.
12. Sellers, J. R., Spudich, J. A., and Sheetz, M. P. (1985) Light chain phosphorylation regulates the movement of smooth muscle myosin on actin filaments, *J. Cell Biol. 101*, 1897−1902.
13. Murakami, N., Chauhan, V. P., and Elzinga, M. (1998) Two nonmuscle myosin II heavy chain isoforms expressed in rabbit brains: Filament forming properties, the effects of phosphorylation by protein kinase C and casein kinase II, and location of the phosphorylation sites, *Biochemistry 37*, 1989−2003.
14. Conti, M. A., Sellers, J. R., Adelstein, R. S., and Elzinga, M. (1991) Identification of the serine residue phosphorylated by protein kinase C in vertebrate nonmuscle myosin heavy chains, *Biochemistry 30*, 966−970.
15. Murakami, N., Healy-Louie, G., and Elzinga, M. (1990) Amino acid sequence around the serine phosphorylated by casein kinase II in brain myosin heavy chain, *J. Biol. Chem. 265*, 1041−1047.
16. Murakami, N., Singh, S. S., Chauhan, V. P., and Elzinga, M. (1995) Phospholipid binding, phosphorylation by protein kinase C, and filament assembly of the COOH terminal heavy chain fragments of nonmuscle myosin II isoforms MIIA and MIIB, *Biochemistry 34*, 16046−16055.
17. Li, Z.-H., Spektor, A., Varlamova, O., and Bresnick, A. R. (2003) Mts1 regulates the assembly of nonmuscle myosin-IIA, *Biochemistry 42*, 14258−14266.
18. Grigorian, M., Tulchinsky, E., Zain, S., Ebralidze, A. K., Kramerov, D. A., Kriajevska, M. V., Georgiev, G. P., and Lukanidin, E. M. (1993) The mts1 gene and control of tumor metastasis, *Gene 135*, 229−238.
19. Ambartsumian, N. S., Grigorian, M. S., Larsen, I. F., Karlstrom, O., Sidenius, N., Rygaard, J., Georgiev, G., and Lukanidin, E. (1996) Metastasis of mammary carcinomas in GRS/A hybrid mice transgenic for the mts1 gene, *Oncogene 13*, 1621−1630.
20. Davies, M. P., Rudland, P. S., Robertson, L., Parry, E. W., Jolicoeur, P., and Barraclough, R. (1996) Expression of the calcium-binding protein S100A4 (p9Ka) in MMTV-neu transgenic mice induces metastasis of mammary tumours, *Oncogene 13*, 1631−1637.
21. Kriajevska, M., Tarabykina, S., Bronstein, I., Maitland, N., Lomonosov, M., Hansen, K., Georgiev, G., and Lukanidin, E. (1998) Metastasis-associated Mts1 (S100A4) protein modulates protein kinase C phosphorylation of the heavy chain of nonmuscle myosin, *J. Biol. Chem. 273*, 9852−9856.

22. Kriajevska, M., Bronstein, I. B., Scott, D. J., Tarabykina, S., Fischer-Larsen, M., Issinger, O., and Lukanidin, E. (2000) Metastasis-associated protein Mts1 (S100A4) inhibits CK2-mediated phosphorylation and self-assembly of the heavy chain of nonmuscle myosin, *Biochim. Biophys. Acta 1498*, 252−263.
23. Jones, T., Zou, J., Cowan, S., and Kjeldgaard, M. (1991) Improved methods for building protein models in electron density maps and the location of errors in these models, *Acta Crystallogr. A47*, 110−119.
24. Collaborative Computational Project, No. 4 (1994) The CCP4 Suite: Programs for Protein Crystallography, *Acta Crystallogr. D50*, 760−763.
25. Guex, N., and Peitsch, M. (1997) SWISS-MODEL and the Swiss-PdbViewer: An environment for comparative protein modeling, *Electrophoresis 18*, 2714−2723.
26. Brunger, A., Adams, P., Clore, G., DeLano, W., Gros, P., Grosse-Kunstleve, R., Jiang, J., Kuszewski, J., Nilges, M., Pannu, N., Read, R., Rice, L., Simonson, T., and Warren, G. (1998) Crystallography & NMR system: A new software suite for macromolecular structure determination, *Acta Crystallogr. D54*, 905−921.
27. Nicholls, A., Sharp, K., and Honig, B. (1991) Protein folding and association: Insights from the interfacial and thermodynamic properties of hydrocarbons, *Proteins 11*, 281−296.
28. Berger, B., Wilson, D. B., Wolf, E., Tonchev, T., Milla, M., and Kim, P. S. (1995) Predicting coiled coils by use of pairwise residue correlations, *Proc. Natl. Acad. Sci. U.S.A. 92*, 8259−8263.
29. Vallely, K. M., Rustandi, R. R., Ellis, K. C., Varlamova, O., Bresnick, A. R., and Weber, D. J. (2002) Solution structure of human mts1 (S100A4) as determined by NMR spectroscopy, *Biochemistry 41*, 12670−12680.
30. Laemmli, U. K. (1970) Cleavage of structural proteins during the assembly of the head of bacteriophage T4, *Nature 227*, 680−685.
31. Perrie, W., and Perry, S. (1970) An electrophoretic study of the low-molecular-weight components of myosin, *Biochem. J. 119*, 31−38.
32. Khrapunov, S., and Brenowitz, M. (2004) Comparison of the effect of water release on the interaction of the *Saccharomyces cerevisiae* TATA binding protein (TBP) with "TATA Box" sequences composed of adenosine or inosine, *Biophys. J. 86*, 371−383.
33. Kwok, S. C., and Hodges, R. S. (2004) Stabilizing and destabilizing clusters in the hydrophobic core of long two-stranded α-helical coiled-coils, *J. Biol. Chem. 279*, 21576−21588.
34. Kagawa, H., Gengyo, K., McLachlan, A. D., Brenner, S., and Karn, J. (1989) Paramyosin gene (unc-15) of *Caenorhabditis elegans*. Molecular cloning, nucleotide sequence and models for thick filament structure, *J. Mol. Biol. 207*, 311−333.
35. Parry, D. A. (1981) Structure of rabbit skeletal myosin. Analysis of the amino acid sequences of two fragments from the rod region, *J. Mol. Biol. 153*, 459−464.
36. McLachlan, A. D., and Karn, J. (1983) Periodic features in the amino acid sequence of nematode myosin rod, *J. Mol. Biol. 164*, 605−626.
37. Nakasawa, T., Takahashi, M., Matsuzawa, F., Aikawa, S., Togashi, Y., Saitoh, T., Yamagishi, A., and Yazawa, M. (2005) Critical Regions for Assembly of Vertebrate Nonmuscle Myosin II, *Biochemistry 44*, 174−183.
38. Kelley, C. A., and Adelstein, R. S. (1990) The 204-kDa smooth muscle myosin heavy chain is phosphorylated in intact cells by casein kinase II on a serine near the carboxyl terminus, *J. Biol. Chem. 265*, 17876−17882.
39. Trybus, K. M. (1991) Assembly of cytoplasmic and smooth muscle myosins, *Curr. Opin. Cell Biol. 3*, 105−111.
40. Rety, S., Sopkova, J., Renouard, M., Osterloh, D., Gerke, V., Tabaries, S., Russo-Marie, F., and Lewit-Bentley, A. (1999) The crystal structure of a complex of p11 with the annexin II N-terminal peptide, *Nat. Struct. Biol. 6*, 89−95.
41. Rustandi, R. R., Baldisseri, D. M., and Weber, D. J. (2000) Structure of the negative regulatory domain of p53 bound to S100B(ββ), *Nat. Struct. Biol. 7*, 570−574.
42. Inman, K. G., Yang, R., Rustandi, R. R., Miller, K. E., Baldisseri, D. M., and Weber, D. J. (2002) Solution NMR structure of S100B bound to the high-affinity target peptide TRTK-12, *J. Mol. Biol. 324*, 1003−1014.
43. Cross, R. A., Geeves, M. A., and Kendrick-Jones, J. (1991) A nucleation−elongation mechanism for the self-assembly of side polar sheets of smooth muscle myosin, *EMBO J. 10*, 747−756.

BI0500776